Neutron-capture gamma-ray study of levels in Ba135 and description of nuclear levels in the interacting-boson-fermion model

Chrien, R. E.; Koene, B. K. S.; Stelts, M. L.; Meyer, R. A.; Brant, Slobodan; Paar, Vladimir; Lopac, Vjera

Source / Izvornik: **Physical Review C - Nuclear Physics, 1993, 48, 109 - 117**

Journal article, Published version
Rad u časopisu, Objavljena verzija rada (izdavačev PDF)

Permanent link / Trajna poveznica: https://urn.nsk.hr/urn:nbn:hr:217:119019

Neutron-capture gamma-ray study of levels in ^{135}Ba and description of nuclear levels in the interacting-boson-fermion model

R. E. Chrien, B. K. S. Koene,* and M. L. Stelts†
Brookhaven National Laboratory, Upton, New York 11973

R. A. Meyer‡
Montgomery College, Takoma Park, Maryland 20850
and Lawrence Livermore National Laboratory, Livermore, California 94550

S. Brant and V. Paar
Department of Physics, Faculty of Science, University of Zagreb, 41000 Zagreb, Croatia

V. Lopac
Faculty of Technology, University of Zagreb, 41000 Zagreb, Croatia
(Received 17 August 1992)

We have performed neutron-capture gamma-ray studies on natural and enriched targets of ^{134}Ba in order to investigate the nuclear levels of ^{135}Ba. The low-energy level spectra were compared with the calculations using the interacting-boson-fermion model (IBFM) and the cluster-vibration model. The level densities up to 5 MeV that are calculated within the IBFM are in accordance with the constant temperature Fermi gas model. From the spin distribution we have determined the corresponding spin cutoff parameter σ and compared it to the prediction from nuclear systematics.

PACS number(s): 25.40.Lw, 27.60.+j, 21.60.Ev

I. INTRODUCTION

The knowledge of level structure at lower and higher energies in nuclei off the line of stability is a growing requirement of both the applied and fundamental research community [1]. These requirements come from several areas; for example, low-energy structure predictions far from stability are needed to solve the problems in cosmochemistry such as the R-process path [2], and the density of levels are needed in reaction cross-section calculations [3]. Near shell closure we can use large-scale shell model calculations to gain a rather detailed understanding of these nuclei [4]. However, going away from closed shell, shell model calculations rapidly exhaust computer capabilities and we must resort to models based on collective phenomena [5,6]. In particular, the interacting boson model [6–9] for even-even nuclei, the interacting boson-fermion model [9–11] for odd-even nuclei, and the interacting boson fermion-fermion model [12] for odd-odd nuclei are convenient for the description of nuclei far from stability.

In the present paper we present a detailed neutron-capture gamma-ray study of the levels of the nucleus ^{135}Ba. The results of neutron-capture gamma-ray experiments are complementary to information from the (d,p) reaction. The direct (d,p) reaction is sensitive to the structure of the wave functions of the final states, whereas resonance capture proceeding through compound-state formation is nonspecific. This feature ensures that all states in a given spin-parity range are observed, provided the experiment comprises a sufficient number of capture states to smooth out the statistical fluctuations of partial radiation widths. Observable depopulation of the capture states proceeds through $E1$ and $M1$ gamma-ray transitions. Thus, when we use even-even targets, the states observed after s-wave capture have spin $\frac{1}{2}$ or $\frac{3}{2}$, and through p-wave capture final states of spins $\frac{1}{2}$, $\frac{3}{2}$, and $\frac{5}{2}$ may be reached. Further spin-parity restrictions can be derived from the variation of primary gamma-ray intensities with the incident neutron energy.

Our neutron-capture gamma-ray measurements comprised three neutron energy regions: the region of thermal capture and discrete s-wave resonances around 100 eV, and two neutron energy windows centered at 2 keV and at 24 keV, where p-wave contributions are expected to become important. The widths of these windows were 0.9 keV and 2.0 keV, respectively. Although the density of capture states is rather low, the number of resonances covered in the ^{134}Ba(n,γ) experiment is sufficient to regard these measurements as reliable probes of the low-spin states in ^{135}Ba. The probability that a $\frac{1}{2}^+$, $\frac{3}{2}^+$, or $\frac{5}{2}^+$ state below 2 MeV of excitation energy was not observably populated through a primary transition at any of the neutron energies is 3% or less.

Prior to our experiment the nucleus ^{135}Ba was studied through the decay of $\frac{5}{2}^+$ ^{135}La [13–15], with the

*Present address: NIKHEF-H, Amsterdam, The Netherlands.
†Present address: Los Alamos National Laboratory, Los Alamos, NM 87545.
‡Present address: Montgomery College, Takoma Park, MD 20850.

^{134}Ba(d,p) reaction [16], with Coulomb excitation [17,18], with the $(n,n'\gamma)$ reaction [19,20], and with the thermal neutron capture [21]. For ^{135}Ba, the beta-decay studies and the Coulomb excitation work were confined to excitations below $\sim$2 MeV. Levels observed in an earlier (n,γ) study can only be identified with (d,p) states if a systematic error of about 15 keV is assumed.

II. EXPERIMENTAL PROCEDURE

The experiment was performed at the High Flux Beam Reactor (HFBR) at Brookhaven National Laboratory (BNL). Quasimonoenergetic neutron beams were provided by filters in a 4-position rotary collimator installed external to the biological shielding of the reactor. The thermal neutron beam was produced with a bismuth single crystal filter. A filter consisting of 188.5 g/cm^2 scandium transmitted a beam with about 70% of the neutrons in a 2-keV group. The FWHM of this neutron window is 0.9 keV with maximum transmission at 2.0 keV. The average flux over a beam area of 7.27 cm^2 at the collimator exit is 6.5×10^6 neutrons/cm^2 sec. The 24-keV filter consisted of 22.86 cm Fe, 36.20 cm A1, and 6.35 cm S. With this arrangement, 98% of the transmitted neutrons are in a group of FWHM$\simeq$2.0 keV with maximum transmission at 24.3 keV. The average flux over a beam area of 7.27 cm^2 is 1.3×10^6 neutrons/cm^2 sec. For further reduction of the thermal flux in the 2-keV and 24-keV experiments a 0.15-cm Cd filter was also interposed in the beam. A detailed description of the filtered beam facility has been given by Greenwood and Chrien [22].

Capture in discrete resonances was studied with the HFBR fast chopper facility. The data were taken with the chopper spinning at 15 000 rpm. At this speed the neutron bursts have a width of 5.0 μs, which leads to a system resolution of 0.23 μs/m at the 49-m station. Two-parameter data of neutron flight time versus gamma-ray energy were stored event by event and subsequently sorted to produce gamma-ray spectra for any specified flight-time interval.

Spectra of primary and low-energy gamma-rays were taken with the detector viewing the target at 90° to the neutron beam. In the course of the experiment four different Ge(Li) detectors were used. Energy resolutions (FWHM) ranged from 5.7 to 9.6 keV at 7.645 MeV and were between 2.0 and 2.5 keV at the ^{60}Co lines.

Target materials were normally packed in thin-walled (1.6 nm) aluminum containers. The target holder for the ^{134}Ba(n,γ) reaction at the fast chopper consisted of two boron-free glass plates in an aluminum frame. Measurements at the fast chopper were done with elemental targets only, since gamma rays not resulting from capture in the studied resonances can be identified by comparison with gamma-ray spectra from off-resonance scans. In the experiments with thermal, 2-keV, and 24-keV neutron beams, the isotropic assignments of gamma rays were determined from the relative intensities observed with enriched and natural targets. Although the detectors were shielded with LiH filters, gamma rays from capture of scattered neutrons in the Ge(Li) detector are present in all spectra. The background spectrum additionally contains capture gamma rays from aluminum, iron, lead, and hydrogen. Since the Ge(n,γ) spectrum is quite dense, some gamma rays may form unresolved doublets with background lines. We therefore routinely checked the enriched-to-natural ratios of background peaks. When an anomalous intensity ratio was found to be attributable to a gamma-ray component from the studied reaction, the background component in the peak was subtracted using the proper enriched-to-natural ratio for that particular contaminant.

Groups of peaks were least-squares fitted by Gaussian shapes on a linear or quadratic background. It was required that the continuous background level change smoothly through the consecutive fitting regions and that no significant "negative peaks" appear. Energies and intensities of high-energy gamma rays were obtained as weighted averages from fits of the full-energy, single-escape, and double-escape peaks. In cases where more than three peaks occurred at consecutive energy spacings of about 511 keV, the smallest number of transitions compatible with the relative peak areas in the sequence was adopted. Thus, we may have missed relatively weak transitions with the three peaks nested inside a sequence.

III. RESULTS AND THE LEVELS OF ^{135}Ba

The physical properties of the target used are given in Table I.

Neutron-capture gamma-ray spectra from enriched and natural targets were measured with thermal neutrons and with 2- and 24-keV filtered beams, and capture in the discrete resonance at 101.8 eV was studied with the fast chopper facility. The measurements were complicated by the presence of a large relative abundance of ^{135}Ba in the enriched target (see Table I). Because the neutron binding energy for the product nucleus ^{136}Ba exceeds the binding energy for ^{135}Ba by 2.1 MeV, the primary gamma rays from ^{134}Ba(n,γ) appear in a rather dense part of the ^{135}Ba(n,γ) spectrum. Also, the ^{135}Ba(n,γ) reaction has a resonance at 104.4 eV with a neutron width comparable to that of the studied 101.8 eV resonance, $\Gamma_n(101.8)=0.150$ eV and was not resolved in the flight-time spectrum. The isotropic assignments of capture gamma rays from this resonance doublet were obtained from comparison with an earlier experiment [23] in which targets enriched in ^{135}Ba were used. The consistency of our data

TABLE I. Physical properties of ^{134}Ba target used in neutron-capture gamma-ray experiments.

Weight (g)	55.111
Chemical form	
Enriched	$Ba(NO_3)_2$
Natural	$Ba(NO_3)_2$
Isotopic Abundance	130 ($<$0.1/0.10)
(% in enriched target/	132($<$0.1/0.09)
% in natural target)	134(59.40/2.42)
	135(22.88/6.59)
	136(6.62/7.81)
	137(3.09/11.32)
	138(8.01/71.66)

with those of Ref. [24] was checked by examining the ^{135}Ba(n,γ) spectra from capture in the 81- and 86-eV resonances.

Energy calibration of the primary gamma transitions was done with respect to N, Al, Fe, and H capture gamma rays. The low-energy spectra were calibrated against secondary gamma rays from the ^{135}Ba(n,γ) reaction [25]. Absolute photon intensities for capture in the 101.8-eV resonance were obtained relative to the absolute intensities given by Chrien *et al.* for the ^{135}Ba(n,γ) 104-eV resonance by correcting the experimental intensities for the different capture rates in the two resonances. The capture rates were calculated from the known resonance parameters [26] with inclusion of multiple scattering corrections. Absolute intensities at the other neutron energies were derived with respect to the 102-eV resonance intensities by normalizing on the summed intensities of the ground-state transitions from the ^{135}Ba levels at 221, 480, 588, 855, and 874 keV. The implicit assumption that the intensities of these gamma rays are independent of the neutron energy is substantiated by the consistent pattern of their relative intensities through the range of neutron energies. The systematic uncertainty in absolute intensities is estimated at about 20%.

The results are shown in Tables II and III. The primary gamma-ray energies have a systematic uncertainty of 0.3 keV in addition to the random errors given in the table. The transition energies are weighted averages of the results at each neutron energy, after correction of primary gamma rays from the filtered-beam experiments by 2.0 and 24.3 keV. The values $E_x+E_\gamma+E_r$ for the five most energetic transitions give the neutron binding energy

$$B_n = 6973.24(22) \text{ keV}$$

with a χ^2 value of 1.3, which is in excellent agreement with the value of 6974(4) keV in the mass tables of Wapstra and Bos [27]. The excitation energies of the calibration levels were taken from our earlier work on ^{135}La decay [14].

The thermal neutron capture in ^{134}Ba was studied earlier by Groshev *et al.* [21]. Besides the poor agreement with our data (Table IV), the final-state energies deduced in Ref. [21] contain a systematic error of 11 keV because of an incorrect determination in the neutron binding energy as $B_n = 6984$ keV. This value was obtained from the assumption that the 6399-keV transition feeds the level at 588 keV (which was actually taken at 585 keV). Our data show a peak near 6399 keV, but from its relative intensity with enriched and natural targets we conclude that it does not belong to the ^{134}Ba(n,γ) reaction.

The final states populated by primary transitions that are observable in *s*-wave capture, at thermal or at the 102-eV resonance, have spin $\frac{1}{2}$ or $\frac{3}{2}$. Since the level spacing in ^{135}Ba at the neutron binding energy is about 250 eV [26], the 2- and 24-keV data represent average capture over a total of about 12 resonances. The ensuing reduction of statistical strength fluctuations is sufficient to separate $E1$ and $M1$ transitions into two distinct intensity bands, but this does not guarantee that the parities of final states can be established. If the averaging occurs

TABLE II. Primary transitions from the ^{134}Ba$(n,\gamma)^{135}$Ba reaction. The transition energies have been evaluated at the neutron binding energy, B_n. The four lowest excitation energies were taken from our study of the decay of ^{135}La [14] and were used to determine B_n. The uncertainties in energies and intensities represent random errors only.

E_x	$E_\gamma+E_r$	$I_\gamma(B_n/E_\gamma)^3$ (photons/100 captures)			
(keV)	(keV)	Thermal	102 eV	2 keV	24 keV
0	6973.5(3)	0.34(4)	1.03(6)	0.51(8)	1.4(3)
220.94	6752.1(7)		0.21(6)	1.0(3)	2.0(5)
480.51	6491.8(5)			0.46(6)	1.3(3)
587.83	6385.5(6)		0.36(6)	1.57(16)	1.8(3)
855.0	6119.7(14)		0.66(10)	1.13(14)	1.1(3)
910.1	6063.1(2)	a	0.38(14)	1.22(19)	2.0(5)
980.2	5993.0(5)			0.61(15)	≤ 1.7[a]
1165.1	5808.1(7)[b]		0.46(17)		≤ 0.3
1211.5	5762.2(9)		0.61(10)	≤ 0.4[a]	1.2(2)
1226.1	5747.1(6)		0.28(9)	0.29(9)	0.3(2)
1584.4	5388.8(2)	9.1(9)	0.95(12)	1.94(13)	0.8(2)
1794.3	5178.9(5)		1.0(2)	0.39(17)	a
1830.0	5143.2(9)		1.1(3)	0.10(12)	0.5(3)
1878.5	5094.7(4)		1.7(6)	0.23(20)	0.6(4)
1971.6	5001.6(4)			0.27(16)	0.9(2)
1997.4	4975.8(9)		1.4(3)	0.74(11)	1.6(8)
2078.6	4894.6(3)	3.8(11)	3.6(5)	≤ 0.7[a]	1.1(3)
2117.7	4855.5(12)		0.7(2)	1.2(5)	0.3(2)
2150.7	4822.5(4)	1.8(3)	a	1.0(2)	2.0(6)
2447.7	4525.5(3)	7.0(6)	a	a	a

[a]Not analyzable due to a dominant contaminant component in the peak.
[b]Questionable assignment.

over both s- and p-wave capturing states, the observed transitions to final states of either parity contain $E1$ and $M1$ components. The values I_γ/E_γ^3 for final states of known spin-parity $\frac{1}{2}^+$ or $\frac{3}{2}^+$ ($E_x=0$, 221, 588, 910 keV) and $\frac{1}{2}^-$ or $\frac{3}{2}^-$ ($E_x=1584$, 1997 keV) are indeed of the same order. The ratio of the means,

$$\frac{\langle I_\gamma/E_\gamma^3(C\rightarrow\frac{1}{2}^+,\frac{3}{2}^+)\rangle}{\langle I_\gamma/E_\gamma^3(C\rightarrow\frac{1}{2}^-,\frac{3}{2}^-)\rangle},$$

has a value close to that estimated from the calculated ratio of the s- and p-wave cross sections, both at the 2- and 24-keV neutron windows. In this estimation we used the empirical rule that $E1$ primary transitions are about 7 times faster than $M1$ transitions [28]. Because of the good agreement between the calculation and experiment in the case of $\frac{1}{2}^-$, $\frac{3}{2}^-$, and $\frac{1}{2}^+$, $\frac{3}{2}^+$ final states, we consider the calculated feeding intensities of $\frac{5}{2}^+$ and $\frac{5}{2}^-$ states from $p_{3/2}$ capture states as realistic estimates. It is found that in the 2-keV experiment the $\frac{5}{2}^+$ states will be populated about 2.5 times weaker than $\frac{1}{2}^+$ and $\frac{3}{2}^+$ states, and at 24 keV both groups of states will be populated with about the same intensity. Transitions to $\frac{5}{2}^-$ states will be below the experimental limit of sensitivity.

In summary, states observably populated in the filtered-beam measurements have $\frac{1}{2}^+$, $\frac{3}{2}^+$, or $\frac{5}{2}^+$ character, but if a state is also populated after pure s-wave capture a $\frac{5}{2}^+$ assignment is ruled out. The increase in the filtered-beam experiments of the population strength of $\frac{1}{2}^+$, $\frac{3}{2}^+$, and $\frac{5}{2}^+$ states to the same magnitude as for $\frac{1}{2}^-$ and $\frac{3}{2}^-$ states, combined with the reduction of statistical strength fluctuations resulting from resonance averaging, allow the conclusion that any low-energy state ($E_x<2$ MeV) not observed in these experiments has a spin-parity value of $\frac{5}{2}^-$ or $>\frac{5}{2}$. In other words, it is unlikely that a low-lying $\frac{1}{2}^+$, $\frac{3}{2}^+$, or $\frac{5}{2}^+$ state has been missed. The probability that the population intensity of such a state was below the experimental sensitivity is estimated at 3%

TABLE III. Secondary gamma rays from the ^{134}Ba(n,γ) ^{135}Ba reaction. (Data from 2- and 14-keV neutron capture are only up to 2.0 MeV.)

Gamma-ray energy	Gamma-ray intensity (photons/100 captures)			
(keV)	Thermal	102 eV	2 keV	24 keV
220.90(15)	10.3(2)	12.9(7)	10.1(2)	10.30(15)
366.58(18)	1.4(2)	1.75(10)	1.63(6)	1.48(12)
374.20(13)	0.93(14)	1.41(10)	1.27(6)	1.41(12)
445.4(4)[a,b]	2.8(3)	3.2(2)	3.0(1)	3.1(3)
480.48(5)	10.5(7)	9.0(2)	10.3(2)	10.6(17)
587.91(5)	6.14(6)	5.52(14)	6.44(7)	5.7(2)
633.86(9)	1.3(3)	1.68(6)	1.83(8)	3.1(5)
637.6(2)[c]		0.45(7)		
690.5(6)		0.89(13)		1.5(2)
720.74(10)[d]	0.34(8)		0.7(3)	0.8(2)
744.90(10)[c]		0.24(3)		
758.3(4)		0.43(9)		
855.19(15)	1.2(2)	1.16(13)	1.4(3)	1.26(12)
874.44(6)	1.7(2)	1.31(11)	1.53(8)	1.9(4)
910.24(3)	2.62(13)	2.27(13)	2.60(8)	2.77(12)
956.23(11)	1.4(3)	0.82(9)	1.2(2)	0.7(3)
980.21(17)	3.3(6)	1.9(3)	1.9(3)	2.9(2)
1003.7(10)[c]		0.14(6)		
1213.63(13)	1.46(12)	1.51(12)	2.2(3)	2.0(4)
1225.8(3)	1.32(12)	1.23(12)	1.8(3)	1.1(3)
1291.3(3)		0.39(7)		
1363.62(6)	4.0(5)	1.7(2)	2.7(2)	2.9(7)
1582(1)[e]	0.6(4)		0.4(4)	<1.1
1830.7(5)				1.1(3)
1856.6(2)[d]		0.49(5)		1.4(3)
1874.4(3)[d]	1.0(2)	0.39(8)	1.9(3)	1.2(4)
2080.0(8)[e]	0.8(7)	0.3(1)		
2142.8(2)[d]	0.84(8)	0.19(7)		
2150.5(8)[c]		0.30(9)		
2447.7(3)	2.6(5)			

[a]This transition was placed in the work of Bondarenko *et al.* [19] (see text).
[b]Wide error margins due to subtraction of a Ge(n,γ) component.
[c]Questionable assignment.
[d]Not placed in the level scheme.
[e]Wide error margins due to subtraction of a ^{135}Ba(n,γ) component.

TABLE IV. Data on thermal neutron capture in ^{134}Ba by Groshev *et al.* [21] in comparison to results of the present work.

$E_\gamma + E_r$ (keV)		$I_\gamma(B_n/E_\gamma)^3$ (photons/100 captures)	
Ref. [21]	Present	Ref. [21]	Present
4520	4525.5	5.1	7.0
4895	4894.6	1.7	3.8
5146	5143.2	≤ 0.8	a
5389	5388.8	6.0	9.1
5810	5808.1	0.7	a
6265	6119.7	≤ 0.7	a
6399	b	0.8	a

[a]Not observed in the thermal spectra.
[b]No gamma ray.

in the 24-keV measurement, and in the 2-keV measurement it is estimated at 3% ($\frac{1}{2}^-, \frac{3}{2}^-$), 5% ($\frac{1}{2}^+, \frac{3}{2}^+$), and 20% ($\frac{5}{2}^+$).

The composite ^{135}Ba level scheme from our decay scheme studies [14,29], the (d,p) reaction [16], Coulomb excitation [18], $(n,n'\gamma)$ excitation [19,20], and our present work is shown in Fig. 1(a). The states at 1794 and 1830 keV have not been observed before. The level at 1165 keV corresponds to the level placed earlier at 1174 keV by Groshev *et al.*, and the level at 1226 keV corresponds to the level placed by Bondarenko *et al.* [19] in their $(n,n'\gamma)$ measurements. New spin-parity restrictions below 1 MeV excitation energy are those for the levels at 717 and 874 keV. The present work excludes $\frac{1}{2}^+$, $\frac{3}{2}^+$, or $\frac{5}{2}^+$ assignments for the 874-keV state. This result selects $\frac{7}{2}^+$ as the correct assignment, which confirms the angular distribution measurements of Dragulescu *et al.* [20] in their $(n,n'\gamma)$ measurements and its strong population in the Coulomb excitation work of Palmer *et al.* [18]. Above 1 MeV, earlier information is only available from the (d,p) study by von Ehrenstein *et al.* [16] and the (n,n') measurements of Bondarenko *et al.* [19]. Our results are compatible with l_n assignments from the (d,p) reaction, and, the narrower spin-parity restrictions from that work are shown (levels at 1445, 1584, 1997, and 2447 keV). Both the 1584- and 2078-keV levels have been assigned as $\frac{3}{2}^-$ by Bondarenko *et al.* It should be noted that we have found no evidence for the 1238-keV level. In our measurements the 2078-keV level has strong population in *s*-wave capture; the transition to this level is

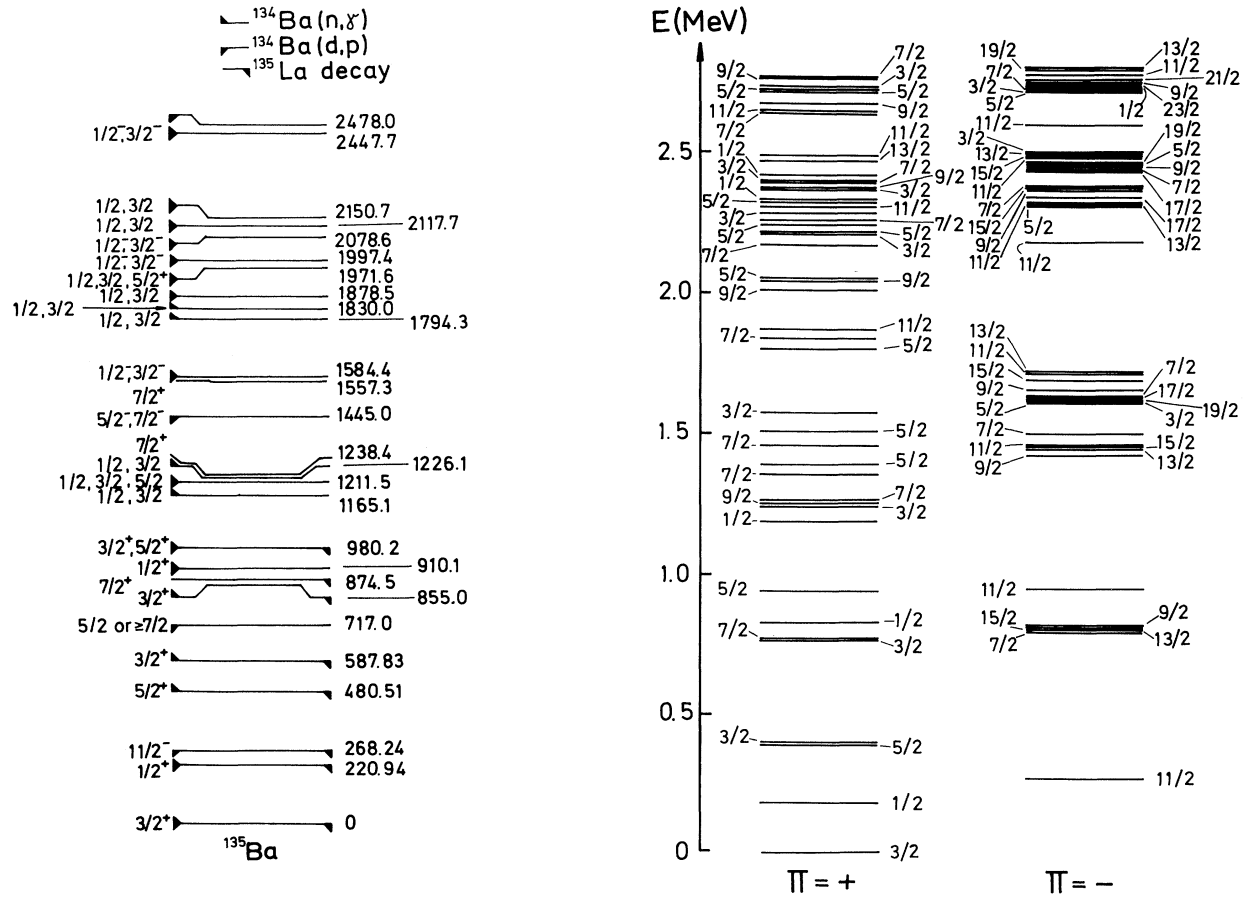

FIG. 1. (a) The level scheme for ^{135}Ba determined from the (n,γ) investigation [note the levels at 268, 717, 874, 1238, 1445, 1557, and 2478 keV were not observed in the (n,γ) investigation but are included to indicate those known levels not observed]. (b) The low-lying levels of ^{135}Ba calculated within IBFM.

dominant in the 102-eV measurement, and at thermal neutron capture, it is of the same magnitude as the $E1$ transitions to the 1584- and 2447-keV levels. The only discrepancy between the (d,p) and (n,γ) data concerns the level at 2151 keV with a tentative $l_n=3$ assignment. From our data we must conclude a spin of $\frac{1}{2}$ or $\frac{3}{2}$. We support the $\frac{7}{2}^+$ assignment for the 1557-keV level proposed by Bondarenko *et al.* because of its absence in our spectra. Also, the level at 1238 keV cannot have $J<\frac{7}{2}$ because of its absence in our spectra and is thus suggested to have a $\frac{7}{2}^+$ value as well. We do not find any evidence for a $\frac{1}{2}^+$ level at 932 keV proposed by Bondarenko *et al.* We note that the $(n,n'\gamma)$ reaction studies of Dragulescu *et al.* do not report any such level either. Further, we do not observe levels at 1871 and 1940 keV that are reported by Bondarenko *et al.* as having spins of $\frac{3}{2}$ or $\frac{5}{2}$. If they exist, then they most likely have $J=\frac{5}{2}$. We do note that we do observe the population of a level at 1879 keV. Similarly, their 1991- and 2075-keV levels, which they assign as $\frac{3}{2}^-$, may correspond to the levels we observe at 1997 and 2075 keV, the latter of which we assign as $\frac{3}{2}^-$. Last, we observe a 445.4(4)-keV gamma ray in all our measurements (thermal, 102 eV, and 2 and 24 keV). Bondarenko *et al.* have identified this gamma ray as being the transition from the first excited $\frac{7}{2}^-$ level to the $\frac{11}{2}^-$ level, thus giving a $\frac{7}{2}^-$ level at 714.2 keV. The observation of this $\frac{7}{2}^-$ level in our neutron-capture gamma-ray measurements is presumably from its population by higher-energy levels which we populate.

No new levels were proposed on the basis of energy sums. Level energies in Fig. 1(a) are from the best simultaneous fit to the gamma-ray placements shown, and for gamma rays we placed in the ^{135}La decay scheme study. No multiple placements were considered since the present gamma-ray branching ratios and those from the decay studies agree. None of the fits appear unrealistic with regard to the spin-parities we propose or the gamma-ray intensity balances. The figure contains no fits to the (d,p) states at 717 and 1445 keV, which have energy uncertainties of ± 10 keV [29].

IV. IBFM DESCRIPTION OF ^{135}Ba

The nuclear structure of ^{135}Ba was described in the framework of the interacting-boson-fermion model (IBFM) [9–11], by coupling a valence-shell neutron quasiparticle to the IBM boson core. In the calculation, we employ the TQM representation [11] of IBM.

The core nucleus ^{134}Ba was described [30] in the O(6) limit [6,8] of IBM, in accordance with the evidence for extensive region of nuclei near $A=130$ resembling the O(6) symmetry [31]. Casten and Brentano [31] have proposed an average parametrization for nuclei near $A=130$; in the calculation for ^{134}Ba their values for the O(6) parameters A,B,C have been scaled using a multiplication factor 1.4. The boson number is $N=5$. In the IBFM calculation we have included the neutron quasiparticle states $d_{3/2}$, $h_{11/2}$, $s_{1/2}$, $g_{7/2}$, and $d_{5/2}$ with energies 0, 0.111, 0.348, 1.660, and 2.315 MeV, and BCS occupation probabilities 0.798, 0.852, 0.910, 0.980, and 0.988, respectively. These values correspond to the BCS solution employing the standard parametrization used by Kisslinger and Sorensen [32], with an additional shift upwards of the $s_{1/2}$ single-particle position by 0.9 MeV, which is in accordance with the low-lying experimental $\frac{1}{2}_1^+$ level in the $N=81$ nucleus ^{137}Ba. The boson-fermion interaction strengths for positive-parity states have the following values [30]: dynamical interaction strength $\Gamma_0=0.05$ MeV, exchange interaction strength $\Lambda_0=1.45$ MeV, monopole interaction strength $A_0=-0.08$ MeV, and the χ value $\chi=0$. For negative parity states we use [30] $\Gamma_0=0.2$ MeV, $\Lambda_0=0.2$ MeV, and $A_0=0$ MeV. In Fig. 1(b) we present the IBFM spectrum up to 2.8 MeV in comparison to the present data.

It should be noted that in the case of $N=79$ nuclei the sign of the ground-state quadrupole moment is a sensitive test of the model. In the IBFM calculation the calculated static quadrupole moment is positive, in agreement with experiment [33]. For the values of effective fermion charge $e^{\text{s.p.}}=0.8$ and effective vibrator charge $e^{\text{vib}}=1.6$ we obtain the ground-state quadrupole moment $Q(\frac{3}{2}_1^+)=+0.10\ e\,\text{b}$. The experimental results for $Q(\frac{3}{2}_1^+)$ are $+0.146(16)\ e\,\text{b}$ [34] and $+0.160(3)\ e\,\text{b}$ [35]. The effective charges used were adjusted [30] to the experimental $B(E2)$ values for transitions between the low-lying states. $B(E2)$ $(\frac{1}{2}_1^+\rightarrow\frac{3}{2}_1^+)=0.019(1)\ e^2\text{b}^2$, $B(E2)$ $(\frac{5}{2}_1^+\rightarrow\frac{1}{2}_1^+)=0.010(2)\ e^2\text{b}^2$ and $B(E2)$ $(\frac{5}{2}_1^+\rightarrow\frac{3}{2}_1^+)=0.119(6)\ e^2\text{b}^2$. The corresponding calculated values are $0.021\ e^2\text{b}^2$, $0.044\ e^2\text{b}^2$, and $0.192\ e^2\text{b}^2$. In the $E2$ operator we have employed the χ term with parameter $\chi=-1$. The negative value of χ corresponds to the negative sign of the measured electric quadrupole moment of the first excited state of the ^{134}Ba core nucleus [33].

The $M1$ properties were calculated employing the values of gyromagnetic ratios $g_R=Z/A$, $g_l=g_l^n(\text{free})=0$, $g_s=0.7g_s^n(\text{free})$. The tensor term in the $M1$ operator was included with the strength [36] $g_T=\frac{1}{100}\ \langle r^2\rangle g_s^{\text{free}}=-0.87$. In particular, the tensor term is needed to describe the $B(M1)$ value for the $\frac{1}{2}_1^+\rightarrow\frac{3}{2}_1^+$ transition, which is l forbidden in the zeroth-order approximation, and therefore strongly hindered without inclusion of the tensor term. The calculated value is $B(M1)(\frac{1}{2}_1^+\rightarrow\frac{3}{2}_1^+)=0.0106\mu_N^2$ and the experimental value is $0.006(4)\mu_N^2$. The calculated magnetic dipole moment of the ground state is $\mu(\frac{3}{2}_1^+)=+0.92\mu_N$ and the experimental value is $+0.838\mu_N$.

The calculation of the nuclear structure of ^{135}Ba was previously performed [20] in the cluster-vibration model (CVM) [37]. A similar calculation was performed for another $N=79$ nucleus, ^{133}Xe [38]. In both CVM calculations a reasonable agreement with experiment was obtained, except for the sign of the ground-state quadrupole moment. In both calculations the calculated sign of $Q(\frac{3}{2}_1^+)$ was negative, in contradiction to experiment. Here, we have performed CVM calculations for the $N=79$ nuclei employing the natural parametrization. The energies of the single holes have been taken as the experimentally deduced centers of gravity obtained from transfer reaction studies and are $e(s_{1/2}^{-1})$-$e(d_{3/2}^{-1})=0.54$ MeV and $e(h_{11/2}^{-1})$-$e(d_{3/2}^{-1})=1.07$ MeV. The phonon en-

ergy has been taken as the average of the energies of the 2_1^+ states in ^{134}Te and ^{132}Te. The standard value has been taken for the pairing strength, $G=20/A$. Thus, the only free parameter in the calculation of the energy spectrum is the particle-vibration coupling strength a. In Fig. 2 we present the calculated CVM spectra as a function of a. These energy spectra are rather similar to the results of IBFM. However, the CVM calculation systematically gives a negative sign [$Q(\frac{3}{2}_1^+)\approx -0.2$ e b], in contradiction to experiment. This result for $Q(\frac{3}{2}_1^+)$ is persistent and rather independent of the details of the parametrization. We have not succeeded in obtaining a correct sign of $Q(\frac{3}{2}_1^+)$ in CVM without seriously distorting the energy spectrum. On the other hand, the IBFM calculation reproduces the correct sign in a natural way.

Finally, let us investigate the level density and spin distribution associated with the present IBFM calculation for ^{135}Ba. The nuclear level densities are usually investigated on the basis of the Fermi gas model and various semiempirical modifications of the Fermi gas formula [39–42]. It has been shown recently that the systematics of experimental level densities in a number of nuclei can be well described by using a constant-temperature Fermi gas model (CTFGM) formula [43]. It has been demonstrated that CTFGM gives a parametrization of the level density in the low-energy region comparable to the conventional backshifted Fermi gas model.

Here we compare the IBFM spectrum of ^{135}Ba to the CTFGM. In the IBFM calculation we employ the parametrization that reproduces reasonably well the low-energy states in ^{135}Ba. We note that statistical analysis of the energy spectra has been recently extended [44–47] to the boson approach to nuclear structure. Now we investigate the density of levels up to 5 MeV obtained with the present IBFM calculations for ^{135}Ba. In the energy region considered, the cumulative number of IBFM levels is of the order of 10^2, which is appropriate for statistical considerations. In Fig. 3 the cumulative number of IBFM levels is shown (by the steplike line denoted a). This IBFM result is fitted by the CTFGM formula:

$$N(E)=\exp\{(E-E_0)/T\}+C$$

which is obtained by integrating the CTFGM level density. Here, E_0 is the ground-state backshift, T is the nuclear temperature, and the integration constant reflects the occurrence of the lowest levels, which are dominated by specific nuclear structure effects and not by statistical correlations.

The CTFGM fit to the IBFM results is shown in Fig. 3 by curve b. The fitted values of CTFGM parameters are

$$T=1.894 \text{ MeV},$$

$$E_0=-6.384 \text{ MeV},$$

$$C=-36.417.$$

In a second step we have considered $N(E)$ within the

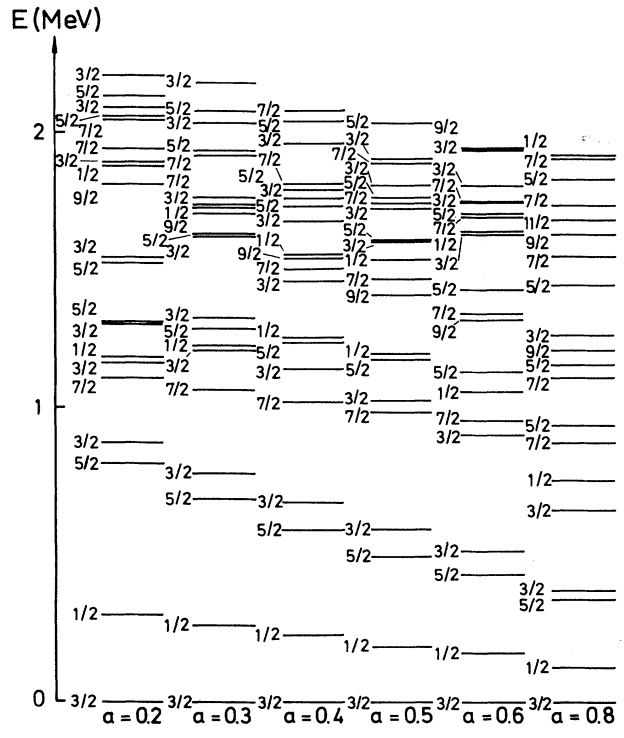

FIG. 2. Calculation of the $N=79$ level spectrum within the cluster-vibration model as a function of the coupling constant a.

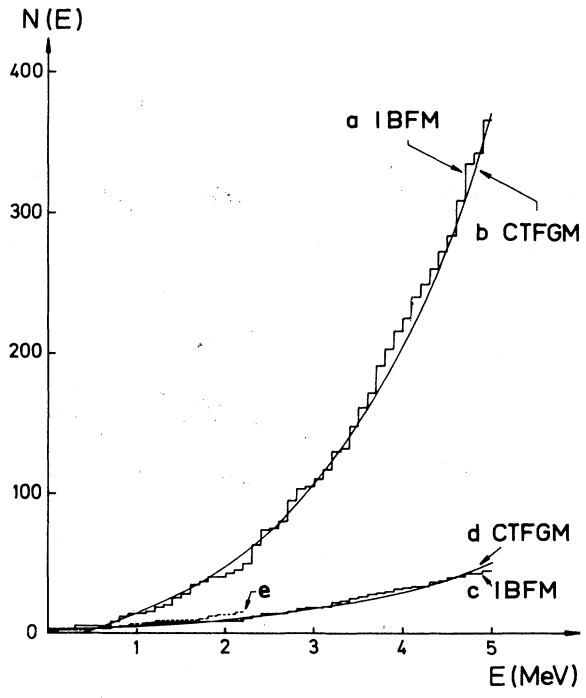

FIG. 3. Cumulative number of the ^{135}Ba levels calculated in IBFM shown in dependence on energy up to 5 MeV. The levels are counted in bins of 100 keV. On the vertical axis we display the total number of levels up to energy E. For comparison, the CTFGM fit to the IBFM level density is shown (see text).

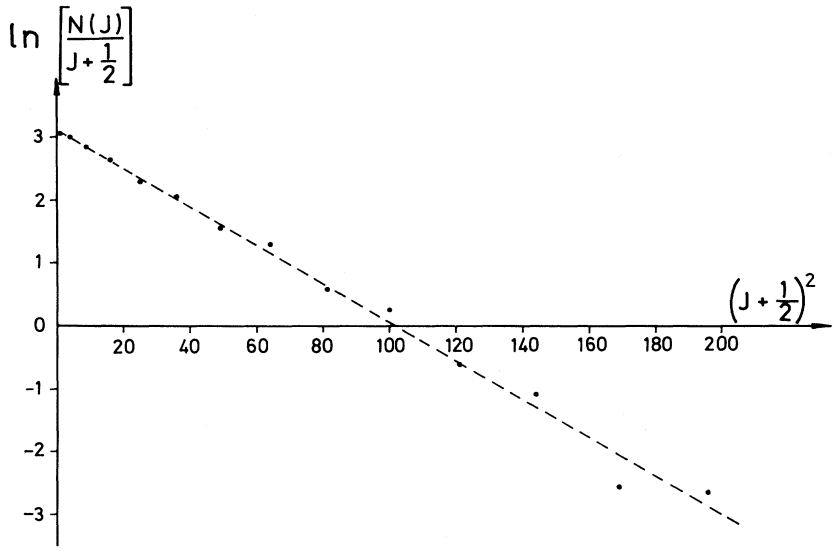

FIG. 4. Spin distribution of the IBFM energy levels of ^{135}Ba up to 5 MeV (closed circles). The horizontal axis displays $(J+\frac{1}{2})^2$ and the vertical $\ln\{N(J)/(J+\frac{1}{2})\}$, where $N(J)$ is the number of states of spin J below 5 MeV. For comparison, the spin distribution given by Bethe formula for the spin cutoff parameter $\sigma=4.048$ is presented (dashed line).

spin window comprising the states with spin-parity values of $\frac{1}{2}^+$ and $\frac{3}{2}^+$. The corresponding IBFM results are displayed in Fig. 3 by the steplike line denoted with the label *c*. The corresponding CTFGM prediction, corresponding to the same values of the parameters T and E_0 as in the case of all spins (curve *b*), is presented as curve *d*. Curve *e* presents the cumulative number of experimentally identified levels of $\frac{1}{2}^+$ and/or $\frac{3}{2}^+$. These CTFGM predictions have been obtained by using the standard spin-dependent formula [43]:

$$N(I,E)=f(I)N(E)+C(I)$$

with the spin distribution function

$$f(I)=\exp\{-I^2(2\sigma)^{-2}\}-\exp\{-(I+1)^2(2\sigma)^{-2}\}$$

where σ is the spin cutoff parameter. From this we have an approximate expression:

$$N(I=\tfrac{1}{2},E)+N(I=\tfrac{3}{2},E)=F\exp\{(E-E_0)/T\}+C'$$

with

$$F=1-\exp\{-3\sigma^{-2}\}\ ,$$

$$C'=C(\tfrac{1}{2})+C(\tfrac{3}{2})\ .$$

The values F and C' have been determined by a fit to the IBFM $(\frac{1}{2}^++\frac{3}{2}^+)$ distribution. Having F, the spin cutoff parameter σ is given by

$$\sigma=\{-3/\ln(1-F)\}^{1/2}\ .$$

In this way we obtain for the $\frac{1}{2}^++\frac{3}{2}^+$ IBFM levels of ^{135}Ba

$$\sigma=4.734,\quad C'=-1.037\ .$$

There is no effect of truncation space below 5 MeV in the sense that there is a good agreement between the IBFM and the CTFGM in this energy range.

In Fig. 4 we present the spin distribution for IBFM levels up to 5 MeV. For comparison, we present in the figure, by a dashed line, the spin distribution given by Bethe formula with the spin cutoff parameter $\sigma=4.048$, obtained by fitting the IBFM spin distribution of all levels up to 5 MeV. The corresponding expression for the average value of the spin cutoff parameter, $\sigma=0.98A^{0.29}$, as determined by von Egidy *et al.* [43] by fitting the experimental spin distributions in 75 nuclides gives $\sigma=4.065$.

V. CONCLUSIONS

Using neutron-capture gamma-ray spectroscopy we have investigated the level scheme of the nucleus ^{135}Ba and compared it with the IBFM calculation. In addition, using the same IBFM calculation, we have determined the level density and spin distribution up to 5 MeV excitation energy and compared it to the constant-temperature Fermi gas model.

[1] *Nuclei Off the Line of Stability,* edited by R. A. Meyer and D. S. Brenner (Am. Chem. Soc., Washington, D.C., 1979).
[2] G. J. Mathews, W. M. Howard, K. Takahashi, and R. A. Ward, in [1], p. 134.
[3] M. A. Gardner and D. G. Gardner, in [1], p. 100.
[4] J. B. McGrory and B. H. Wildenthal, Annu. Rev. Nucl. Part. Sci. **30**, 383 (1980).
[5] A. Bohr and B. R. Mottelson, *Nuclear Structure* (Benja-

min, New York, 1975), Vol. II.
[6] F. Iachello and A. Arima, *The Interacting Boson Model* (Cambridge University Press, Cambridge, 1987).
[7] A. Arima and F. Iachello, Phys. Rev. Lett. **35**, 157 (1975).
[8] A. Arima and F. Iachello, Ann. Phys. (N.Y.) **123**, 468 (1979).
[9] F. Iachello and O. Scholten, Phys. Rev. Lett. **43**, 679 (1979).
[10] O. Scholten, thesis, University of Groningen, 1980.
[11] V. Paar, Inst. Phys. Conf. Ser. **49**, 53 (1980); V. Paar, S. Brant, L. F. Canto, G. Leander, and M. Vouk, Nucl. Phys. **A378**, 41 (1982).
[12] V. Paar, in *Capture γ-Ray Spectroscopy and Related Topics,* edited by S. Raman (American Institute of Physics, New York, 1985), p. 70; S. Brant, V. Paar, and D. Vretenar, Z. Phys. A **319**, 355 (1984); V. Paar, D. K. Sunko, and D. Vretenar, *ibid.* **327**, 291 (1987).
[13] S. Morinobu, T. Hirose, and K. Histake, Nucl. Phys. **61**, 613 (1965).
[14] F. Bazan and R. A. Meyer, Nucl. Phys. **A164**, 552 (1971).
[15] R. B. Begzhanov, D. A. Gladyshev, O. S. Kobilov, P. S. Radzhapov, and K. S. Sabirov, Bull. Acad. Sci. USSR, Phys. Ser. **35**, 2312 (1972).
[16] D. von Ehrenstein, G. C. Morrison, J. A. Nolen, and N. Williams, Phys. Rev. C **1**, 2066 (1970).
[17] D. G. Alkhazov, K. I. Erokhina, and I. K. Lemberg, Bull. Acad. Sci. USSR, Phys. Ser. **27**, 1339 (1964).
[18] D. C. Palmer, R. C. Morgan, J. R. Cresswell, P. D. Forsyth, I. Hall, M. Maynard, and D. J. Thomas, J. Phys. G **2**, 421 (1976).
[19] V. A. Bondarenko, I. L. Kuvaga, P. T. Prokof'ev, G. L. Rezvaya, and T. L. Solomonova, Izv. Akad. Nauk CCCP **47**, 2089 (1983).
[20] E. Dragulescu, M. Ivascu, R. Mihu, D. Popescu, G. Semenescu, A. Velenik, and V. Paar, J. Phys. G **10**, 1099 (1984).
[21] L. V. Groshev, V. N. Dvoretskii, A M. Demidov, and M. S. Alvash, Yad. Fiz. **10**, 681 (1969) [Sov. J. Nucl. Phys. **10**, 392 (1970)].
[22] R. C. Greenwood and R. E. Chrien, Nucl. Instrum. Methods **138**, 125 (1976).
[23] W. Gelletly, J. A. Moragues, M. A. Mariscotti, and W. R. Kane, Phys. Rev. C **1**, 1052 (1970).
[24] D. G. Sarantites, G. E. Gordon, and C. D. Coryell, Phys. Rev. **138**, B353 (1965).
[25] R. E. Chrien, D. I. Garber, J. L. Holm, and K. Rimawi, Phys. Rev. C **9**, 1839 (1974).
[26] S. F. Mughabghab and D. I. Garber (compilers), Neutron Cross Sections, Brookhaven National Laboratory Report No. BNL-325, 1973; *Resonance Parameters,* 3rd ed., Vol. I (National Technical Information Service, Springfield, Virginia, 1973).
[27] A. H. Wapstra and K. Bos, At. Data Nucl. Data Tables **19**, 175 (1977).
[28] M. Kortelahti, T. Komppa, M. Piiparinen, A. Pakkanen, and R. Komu, Phys. Scr. **27**, 166 (1983).
[29] R. L. Bunting, Nucl. Data Sheets **15**, 335 (1975).
[30] V. A. Bondarenko, J. L. Kuvaga, P. T. Prokofjev, V. A. Khitrov, Yu. V. Kolnov, Le Hong Khiem, Yu. P. Popov, A. M. Sukhovoj, S. Brant, V. Paar, and V. Lopac, Nucl. Phys. **A551**, 54 (1993).
[31] R. F. Casten and P. von Brentano, Phys. Lett. **152B**, 22 (1985).
[32] L. S. Kisslinger and R. A. Sorensen, Rev. Mod. Phys. **35**, 853 (1963).
[33] P. Raghavan, At. Data Nucl. Data Tables **42**, 189 (1989).
[34] A. C. Mueller, F. Buchinger, W. Klempt, E. W. Otten, R. Neugart, C. Ekström, and J. Heinemeier, Nucl. Phys. **A403**, 234 (1983).
[35] K. Wendt, S. A. Ahmad, C. Ekström, W. Klempt, R. Neugart, and E. W. Otten, Z. Phys. A **329**, 407 (1988).
[36] V. Paar and S. Brant, Nucl. Phys. **A300**, 96 (1978); Phys. Lett. **74B**, 297 (1978).
[37] V. Paar, Nucl. Phys. **A211**, 29 (1973).
[38] V. Paar and B. K. S. Koene, Z. Phys. A **279**, 203 (1976).
[39] H. A. Bethe, Rev. Mod. Phys. **9**, 69 (1937).
[40] T. Ericson, Nucl. Phys. **11**, 481 (1959).
[41] E. Erba, V. Facchini, and E. Saetta-Menichella, Nuovo Cimento **22**, 1237 (1961).
[42] A. Gilbert and A. G. W. Cameron, Can. J. Phys. **43**, 1446 (1965).
[43] T. von Egidy, A. N. Behkami, and H. H. Schmidt, Nucl. Phys. **A454**, 109 (1986).
[44] V. Paar and D. Vorkapić, Phys. Lett. B **205**, 7 (1988).
[45] V. Paar, D. Vorkapić, S. Brant, H. Seyfarth, and V. Lopac, in *Nuclear Structure of the Zirconium Region,* edited by J. Eberth, R. A. Meyer, and K. Sistemich (Springer-Verlag, Berlin, 1988), p. 184.
[46] Y. Alhassid, A. Novoselsky, and N. Whelan, Phys. Rev. Lett. **65**, 2971 (1990).
[47] T. Mizusaki, N. Yoshinaga, and T. Shigehara, Phys. Lett. B **269**, 6 (1991).